



Role of the Prestructured Surface Cloud in Crystal Nucleation

Wolfgang Lechner,¹ Christoph Dellago,² and Peter G. Bolhuis¹

¹*Van 't Hoff Institute for Molecular Sciences, PO Box 94157, 1090 GD Amsterdam, The Netherlands*

²*Faculty of Physics, University of Vienna, Boltzmannngasse 5, 1090 Vienna, Austria*

(Received 16 December 2010; published 22 February 2011)

For the homogeneous crystal nucleation process in a soft-core colloid model, we identify optimal reaction coordinates from a set of novel order parameters based on the local structure within the nucleus, by employing transition path sampling techniques combined with a likelihood maximization of the committor function. We find that nucleation is governed by solid clusters that consist of an hcp core embedded within a cloud of surface particles that are highly correlated with their nearest neighbors but not ordered in a high-symmetry crystal structure. The results shed new light on the interpretation of the surface and volume terms in classical nucleation theory.

DOI: 10.1103/PhysRevLett.106.085701

PACS numbers: 64.70.pv, 81.10.Aj

Homogeneous nucleation of a crystal from the supercooled melt is a phenomenon of great importance in numerous areas of physical science ranging from materials science to biophysics. While this process is well understood on a qualitative level, its atomistic details often remain elusive. In particular, finding a reaction coordinate (RC) that captures the essential physics of the transition mechanism is an open problem with a century-old history. A first phenomenological description of the nucleation mechanism and kinetics was given by the classical nucleation theory (CNT) [1,2], which asserts that the phase transition occurs via the formation and subsequent growth of a solid nucleus of spherical shape. Here, the sole RC is the radius R of the crystalline nucleus leading to the Gibbs free energy (FE)

$$\Delta G(R) = \frac{3}{4} \pi R^3 \Delta \mu + 4 \pi R^2 \gamma, \quad (1)$$

where $\Delta \mu$ is the difference in the chemical potential between metastable liquid and the thermodynamically stable solid phase, and γ is the surface FE of the interface between solid and liquid. CNT has been widely used and successfully applied for decades; however, computer simulations indicate that Eq. (1) misses important details about the freezing transition of soft particles [3].

How can one measure the quality of a RC? Given two metastable states, A (e.g., the liquid phase) and B (e.g., the solid phase), separated by a FE barrier, the perfect RC is the committor function $p_B(\mathbf{x})$, the probability that dynamical trajectories initiated at configuration \mathbf{x} , consisting of the positions of all particles, actually reach the crystalline phase B [4,5]. This function provides a quantitative measure for the progress of a reaction in the sense that it tells us what is likely to happen next [4,6]. However, computing the committor directly requires sampling a large number of trajectories and moreover does not yield any new insight into the nucleation mechanism. Instead, what we seek is a low dimensional representation $p_B[\mathbf{q}(\mathbf{x})]$, in which the

committor depends only on n collective variables (CV) $\mathbf{q}(\mathbf{x}) = \{q_1(\mathbf{x}), q_2(\mathbf{x}), \dots, q_n(\mathbf{x})\}$, which are functions of the particle positions \mathbf{x} . These n CVs should hold all relevant information about the reaction and provide a physically transparent picture of the mechanism. The quality of the RC expressed in terms of the CVs can be evaluated by computing the committor distribution for configurations at a fixed value of the RC. For instance, configurations corresponding to the top of the barrier predicted by Eq. (1), are expected to lead to committor values of $p_B = 0.5$. However, our simulations show that the p_B distribution of 100 independent configurations taken from the top of the barrier [see Fig. 3] is flat rather than sharply peaked at $\frac{1}{2}$, indicating that the size of the crystalline nucleus is not sufficient to describe the transition, and additional variables, such as structure or shape, need to be included to predict the likely fate of a given nucleus. Indeed, based on extensive transition path sampling simulations, Moroni and co-workers [3] suggested as a better RC for the nucleation of a Lennard-Jones system a combination of the nucleus size N and the order parameter (OP) $Q_{6,cl}$, which can be interpreted as the crystallinity of the nucleus. Recently, Kawasaki and Tanaka [7] showed that the nucleus of colloidal hard spheres forms within a region of particles in a preordered random hexagonal close packed structure. In both cases, the assumptions underlying CNT break down demanding an extension of the basic picture provided by CNT.

In this study, we use a new computational technique [8,9] and new structural OPs to find optimal RCs for crystal nucleation, in terms of a low dimensional set of CVs. To find such a low dimensional representation we make use of the recently developed method to extract nonlinear RCs from the reweighted path ensemble (RPE) [8,9]. This method is based on calculating the likelihood that a given representation follows an ideal committor function, which serves as a measure for the quality of the OPs and allows for a systematic evaluation of RCs without any *a priori*

assumptions about the mechanism. As a model system, we will investigate the Gaussian core model, which reproduces the effective interaction of soft-core colloids [10–12]. We show that in contrast to the single variable FE profile predicted by CNT, an optimum RC can only be obtained by including information on both surface and volume independently. The optimal RC suggests a more general form of the classical theory, in which the volume term is interpreted as arising from “core” particles that exhibit a high symmetry crystal structure and the surface term describing particles that are correlated to the structure of their neighbors but not ordered in a crystal structure.

Any study on crystallization requires a suitable definition of OPs that can distinguish the liquid from the solid. The most widely used solid-liquid distinction, due to ten Wolde and Frenkel [13], considers the correlation $S_{ij} = \sum_{m=-6}^6 q_{6m}(i)q_{6m}^*(j)$ between two neighboring particles based on the Steinhardt bond order parameters $q_{lm} = \frac{1}{n_{nb}(i)} \sum_{j=1}^{n_{nb}(i)} Y_{lm}(\mathbf{r}_{ij})$, where Y_{lm} are the spherical harmonics functions, and $n_{nb}(i)$ is the number of nearest neighbors of particle i [14]. In a perfect solid $S_{ij} = 1$; in a liquid this correlation vanishes. Subsequent cluster analysis of connected solidlike particles yields N_{lf} , the number of particles in the largest cluster. In this scheme, a structural analysis of the solid region requires additional steps [15].

Here, we suggest a novel definition of solidity. Lechner and Dellago [16] introduced OPs that allow for an accurate distinction between crystal structures by including information of the second shell neighbors as well. Here, the structural identity of each particle is determined by the largest probability in the reference distributions in Fig. 1 for that particle’s instantaneous \bar{q}_4 and \bar{q}_6 . A particle is

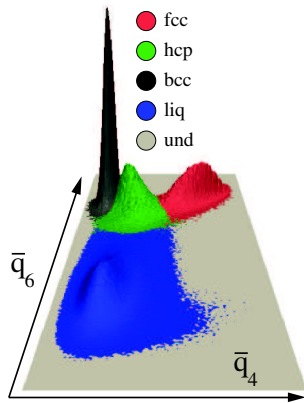


FIG. 1 (color online). Probability distribution in the $\bar{q}_4\bar{q}_6$ plane of crystals in the perfect fcc (red), bcc (black) and hcp (green) structures as well as of the liquid phase (blue) at pressure $P = 0.011$ and temperature $T = 0.0030$. The bond order parameters q_{lm} are averaged over \bar{n}_{nb} , the nearest neighbors of particle i plus particle i itself, $\bar{q}_{lm}(i) = [1/\bar{n}_{nb}(i)] \sum_{k=0}^{\bar{n}_{nb}(i)} q_{lm}(k)$. The inner products of \bar{q}_{4m} and \bar{q}_{6m} are denoted as \bar{q}_4 and \bar{q}_6 , respectively [16]. The joint distributions of these two OPs have a small overlap allowing for an accurate distinction between different crystal structures.

defined as solidlike if it is not within the liquid region in Fig. 1. In other words, the probability to find the local structure of a solidlike particle is vanishing in the undercooled liquid. This method allows one to determine the size N_{ld} of the largest cluster of solidlike particles and its crystal structure in a single step.

We construct several CVs that serve as candidates for the best RC. In addition to N_{ld} we also calculate the size N_{lf} of the largest cluster determined according to the criterion of ten Wolde and Frenkel [13]. With the information about the structure of the particles within the cluster we define the ratio of bcc particles within the cluster n_{bcc} , the ratio of fcc particles n_{fcc} , of hcp particles n_{hcp} , and of particles with undefined structure n_{und} . We also introduce corresponding ratios for the entire system s_{bcc} , s_{fcc} , s_{hcp} , and s_{und} . Further we consider $Q_{6,cl}$ and $Q_{4,cl}$ averaged over all particles in the cluster as suggested in Ref. [3]. The number of liquidlike particles with at least one neighbor in the cluster, N_s , and the total number of connections between these particles and cluster particles, N_l , are also considered. These CVs are now used as candidates for enhancing the original description of the nucleation process based solely on the size of the largest cluster N_{ld} .

Based on the original likelihood maximization scheme developed by Peters and Trout [17] we developed a method that selects the optimal CVs and yields the best nonlinear parametrization of the RC by taking into account the full nucleation process (for details see Ref. [9]). This method takes the RPE [8] as the input data set, which is obtained from a replica exchange transition interface sampling simulation, followed by reweighting all configurations from all paths to their equilibrium weights $w(\mathbf{x})$. Assuming a model committor function $p_B^{est}(r) = 0.5[1 - \tanh(r)]$, the log-likelihood $\ln L = \sum_{\mathbf{x}_A} w(\mathbf{x}_A) \times \ln p_A^{est}(r) + \sum_{\mathbf{x}_B} w(\mathbf{x}_B) \ln p_B^{est}(r)$, where $p_A^{est} = 1 - p_B^{est}$ and $r[\mathbf{q}(\mathbf{x})]$ is the RC model [9]. The first sum goes over all configurations \mathbf{x}_A that are part of RPE paths that end in A weighted by $w(\mathbf{x}_A)$, the second sum accordingly over all configurations that end in B . We allow for nonlinear mapping from $\mathbf{q}(\mathbf{x})$ to r by projecting each configuration \mathbf{x} in the RPE onto a string [18] between A and B in the n -dimensional CV space. This leads to a parameter $\alpha \in [0, 1]$, denoting the progress along the string, which is mapped to r by a monotonic function $r(\alpha)$. Using a Monte Carlo annealing scheme, we maximize the log likelihood $\ln L$ with respect to (i) the string, (ii) the mapping function $r(\alpha)$, and (iii) a relative scaling s of the CVs [9].

We study the nucleation at moderate undercooling in the high as well as the low pressure regime of the Gaussian core model [see phase diagram in Fig. 2]. The simulation details are as follows. The equations of motion are integrated with the velocity Verlet algorithm and temperature and pressure are fixed with the Andersen thermostat and the Andersen barostat, respectively. The pair interaction between the particles is $v(r) = \epsilon \exp(-r^2/\sigma^2)$. Temperatures are given in units of $T^* = k_B T/\epsilon$, distances

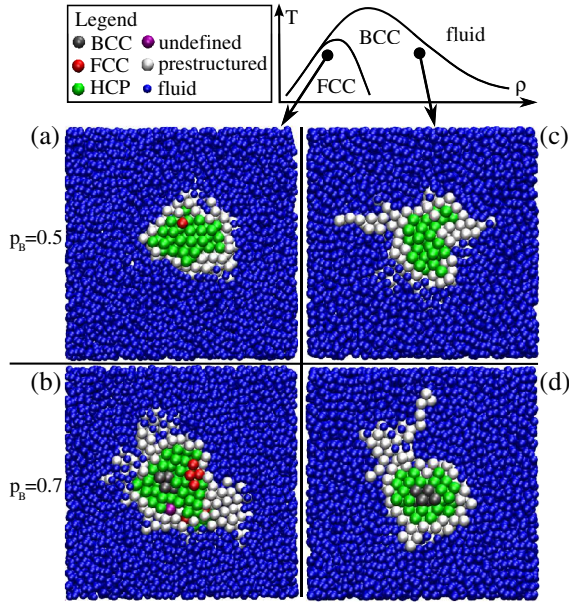


FIG. 2 (color online). Top panel: Schematic phase diagram adapted from Ref. [11]. Lower panels: Cross sections of clusters in the high (right) and low (left) pressure regime: (a) critical cluster in the fcc region consisting almost exclusively of hcp particles (green) surrounded by preordered particles (white); (b) in the postcritical cluster some parts of the core rearrange to fcc or bcc; (c) in the high pressure regime the critical clusters are also mainly of hcp structure; (d) postcritical clusters at high densities rearrange to bcc, predominantly in the center.

in units of $r^* = r/\sigma$, and pressures in units of $P^* = P/(\beta\sigma^3)$. We consider two phase points: the high pressure regime at $P = 1.0$ and $T = 0.0018$, which results in a density of about $\rho = 0.6$ and the bcc structure as the most stable phase, and the low pressure regime at $P = 0.011$ and $T = 0.003$ with a density of approximately $\rho = 0.12$ and fcc as most stable structure. These phase points have been chosen such that the FE barrier of the liquid-solid transition, calculated in preliminary NPT Monte Carlo umbrella sampling simulations, has about the same height in both cases. The number of particles is $N = 10976$ and periodic boundaries are used. The stable states A and B are defined as $N_{ld} \leq 5$ and $N_{ld} \geq 400$, respectively. In order to sample the full trajectory space using replica exchange transition interface sampling simulations [8] we collect both forward paths (that start in A) and backward paths (that start in B) with interfaces at positions $N_{ld} = 10, 20, 40, 60, 80, 100, 160,$ and 200 and at $N_{ld} = 360, 320, 280, 240, 200, 160, 100,$ and 80 , respectively. A total of $N_p = 16 \times 7000$ paths are sampled with a shooting acceptance probability of $P_{acc} \approx 0.4$.

We performed the nonlinear RC optimization with the RPE data set for pairs (q_1, q_2) of CVs where $q_1 = N_{ld}$ and q_2 is one of the above 15 CVs. Figure 3(a) shows the nine-point string and the function $r(\alpha)$ after 20 000 optimization steps on top of the FE contour plot with the transition state indicated as a grey (green) line. Whether or not adding q_2 does enhance the RC is decided by the Bayesian

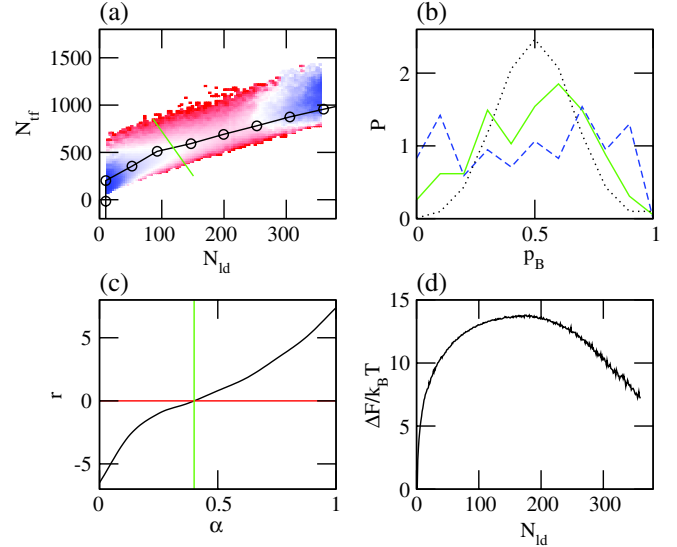


FIG. 3 (color online). (a) Color map of the FE as a function of N_{tf} and N_{ld} for the high pressure regime with the optimized nine-point string (circles). The optimized scaling between N_{tf} and N_{ld} is $s = 0.323$. (b) Comparison of the committor distributions from the transition state (green) and the top of the FE barrier as function of N_{tf} (dashed blue) together with the binomial distribution (dotted) [23]. (c) Mapping function $r(\alpha)$. The transition state is at $\alpha = 0.439$ indicated by the (green) line in the inset and at $N_{tf} = 1588 - 8.5N_{ld}$ in the main graph. (d) One-dimensional projection of the free energy as a function of N_{ld} .

information criterion [19], stating that for each extra model dimension the log likelihood has to increase at least by $b = 1/2 \ln N_d$, where N_d is the sum of all weights over all configurations [8]. We introduce the relative likelihood change $g = [\ln L(q_1, q_2) - \ln L(q_1)]/b$ and the error $\sigma = \langle (g - \langle g \rangle)^2 \rangle^{1/2}$ estimated from six optimizations runs. In both the high and low pressure regime, the pair (N_{ld}, N_{tf}) results in the largest information gain ($g_{high} = 2.35(\sigma = 0.23)$ and $g_{low} = 2.23(\sigma = 0.12)$) while all other OPs lead to a gain smaller than 1 within the error bars. Indeed, the committor distribution along the transition state $r = 0$ [grey (green) line in Fig. 3(c)] is peaked around $p_B = 0.5$ in contrast to the transitions state defined by constant N_{tf} at the top of the FE barrier [see Fig. 3(b)]. Adding a third CV to the model did not improve the RC.

The results of the RC optimization point to a particular role of the particles near the crystal-liquid interface. N_{tf} is the size of the largest cluster in the system consisting of solidlike particles based on the criterion that its local structure is correlated with that of its nearest neighbors [see Fig. 2, white spheres]. The variable N_{ld} , on the other hand, is the size of the largest cluster of solidlike particles by means of the reference distribution in the $\bar{q}_4\bar{q}_6$ plane [Fig. 1]. The cluster defined by the latter is smaller than the N_{tf} cluster [see Fig. 2 (red, green, and black) spheres] and is positioned in the center of the N_{tf} cluster. This core consists of different crystal structures depending on the progress of the nucleation and the state point. In the low

pressure regime the core is primarily of hcp structure even at postcritical cluster sizes, at which vanishingly small fcc and bcc regions develop. The high pressure clusters also start as hcp clusters but then, in a second step, the inner core transforms to the more stable bcc phase, an example of Ostwalds step rule.

The interpretation of the two contributions N_{ld} and N_{tf} sheds new light on the applicability of CNT. The CNT predicts the FE difference with high accuracy in many systems even though the clusters found in simulations are not spherical objects. Consider, now, CNT in a slightly more general form without relying on the assumption of a spherical nucleus: $\Delta G = \Delta\mu N_{\text{core}} + \epsilon_s N_{\text{surface}}$, where ϵ_s is the surface energy, and N_{core} and N_{surface} are the number of particles in the core and in the surface, respectively. We now interpret $N_{\text{core}} = N_{\text{ld}}$ and $N_{\text{surface}} = N_{\text{tf}} - N_{\text{ld}}$. This leads to a FE difference of $\Delta G = c_1 + c_2 N_{\text{ld}} + c_3 N_{\text{tf}}$, where c_i are constants. In the special case $N_{\text{tf}} = k_0 + k_1 N_{\text{ld}} + k_2 N_{\text{ld}}^{(2/3)}$ one recovers the scaling of the FE predicted by CNT. For the system studied here we indeed find $N_{\text{tf}} = 64 + 18N_{\text{ld}}^{0.68}$ even though neither the surface cloud nor the core is of spherical shape. This deviation from a sphere can be measured by the slope of the volume-to-skin ratio ($N_V/N_S = k_1 + k_2 N_V^k$), where the skin consists of particles that have at least one nearest neighbor in the cluster but are not part of the cluster themselves. For perfect spheres of fcc structure $k = 0.43$ for small clusters of size 1–400. The cluster of core particles exhibits $k = 0.37$ and the surface cloud $k = 0.26$, implying that the surface cloud is much rougher than the core. Clearly, the assumption of a spherical cluster does not hold, and the surface cloud and core actually do not even scale in the same way. Nevertheless, the ratio between surface cloud and volume term is equivalent to that of CNT with the interpretation of N_{ld} as volume and $N_{\text{tf}} - N_{\text{ld}}$ as surface. Hence, CNT should predict a correct FE profile for all systems with this scaling of N_{tf} to N_{ld} even without the assumption of spherical clusters. In the system studied here, the fit parameter $c_2 \approx -0.2$ in the high and the low pressure regime, which corresponds well with $\Delta\mu$ in Fig. 2 of Ref. [12].

In summary, we used transition path sampling methods and RC analysis employing a likelihood maximization in combination with a nonlinear string to describe the nucleation in terms of structural properties. Using a set of novel CVs to distinguish between crystal structures reveals that the crystalline cluster forms within a cloud of correlated but unordered particles. Two OPs, the size of the cloud (N_{tf}) and the size of the crystalline core (N_{ld}) are important for the growth of the nucleus. This is in agreement with previous findings [3] suggesting a combination of N_{tf} and $Q_{6,\text{cl}}$, where the latter is basically the cluster crystallinity. A similar conclusion was drawn from studies on hard spheres at densities far beyond the classical nucleation regime that show how crystallization is mediated by low symmetry clusters [20]. Including the particular type of crystalline structure of the core does not improve the RC,

indicating that the rearrangement of the inner core from hcp to bcc in the high pressure regime is a step that is independent of the nucleation. In both pressure regimes the dominant structure is hcp in agreement with Ref. [7,21]. The system investigated here serves as a model for colloidal particles and soft repulsive particles in general and we expect that our approach is applicable to diverse materials ranging from atomic and molecular crystals to colloidal soft matter. Note that our approach is also directly applicable to experimental nucleation trajectory data as obtained, for instance, from confocal microscopy measurements [22].

This work is part of the research program of the Foundation for Fundamental Research on Matter (FOM), which is part of the Netherlands Organization for Scientific Research (NWO) and financially supported by the Austrian Science Foundation (FWF) within the SFB ViCoM (F 41).

-
- [1] R. Becker and W. Döring, *Ann. Phys.* **416**, 719 (1935).
 - [2] K. Binder, *Rep. Prog. Phys.* **50**, 783 (1987).
 - [3] D. Moroni, P. Rein ten Wolde, and P.G. Bolhuis, *Phys. Rev. Lett.* **94**, 235703 (2005).
 - [4] W. E. W. Ren, and E. Vanden-Eijnden, *Chem. Phys. Lett.* **413**, 242 (2005).
 - [5] P.G. Bolhuis, C. Dellago, and D. Chandler, *Proc. Natl. Acad. Sci. U.S.A.* **97**, 5877 (2000).
 - [6] R. B. Best and G. Hummer, *Proc. Natl. Acad. Sci. U.S.A.* **102**, 6732 (2005).
 - [7] T. Kawasaki and H. Tanaka, *Proc. Natl. Acad. Sci. U.S.A.* **107**, 14036 (2010).
 - [8] J. Rogal *et al.*, *J. Chem. Phys.* **133**, 174109 (2010).
 - [9] W. Lechner *et al.*, *J. Chem. Phys.* **133**, 174110 (2010).
 - [10] F.H. Stillinger, *J. Chem. Phys.* **65**, 3968 (1976).
 - [11] S. Prestipino, F. Saija, and P. V. Giaquinta, *Phys. Rev. E* **71**, 050102(R) (2005).
 - [12] S. Prestipino, F. Saija, and P. V. Giaquinta, *J. Chem. Phys.* **123**, 144110 (2005).
 - [13] P. Rein ten Wolde, Maria J. Ruiz-Montero, and D. Frenkel, *J. Chem. Phys.* **110**, 1591 (1999).
 - [14] P.J. Steinhardt, D.R. Nelson, and M. Ronchetti, *Phys. Rev. B* **28**, 784 (1983).
 - [15] J.-M. Leyssale, J. Delhommelle, and C. Millot, *J. Chem. Phys.* **122**, 104510 (2005).
 - [16] W. Lechner and C. Dellago, *J. Chem. Phys.* **129**, 114707 (2008).
 - [17] B. Peters and B.L. Trout, *J. Chem. Phys.* **125**, 054108 (2006); B. Peters, G.T. Beckham, and B.L. Trout, *J. Chem. Phys.* **127**, 034109 (2007).
 - [18] W. E. W. Ren, and E. Vanden-Eijnden, *Phys. Rev. B* **66**, 052301 (2002).
 - [19] G. Schwarz, *Ann. Stat.* **6**, 461 (1978).
 - [20] T. Schilling *et al.*, *Phys. Rev. Lett.* **105**, 025701 (2010).
 - [21] J. Zhu *et al.*, STS-37 Space Shuttle Crew; W.B. Russel and P.M. Chaikin, *Nature (London)* **387**, 883 (1997).
 - [22] U. Gasser *et al.*, *Science* **292**, 258 (2001).
 - [23] B. Peters, *J. Chem. Phys.* **125**, 241101 (2006).